ISSN 1070-3284, Russian Journal of Coordination Chemistry, 2017, Vol. 43, No. 8, pp. 491–499. © Pleiades Publishing, Ltd., 2017.
Original Russian Text © E.O. Platonova, A.P. Pushkarev, V.A. Ilichev, E.V. Baranov, T.A. Kovylina, L.N. Bochkarev, 2017, published in Koordinatsionnaya Khimiya, 2017, Vol. 43, No. 8, pp. 451–459.

Cyclometallated Iridium(III) Complex with 1-Phenylisoquinoline and Norbornene-Substituted Pyrazolonate Ligands and Related Electroluminescent Polymers

E. O. Platonova, A. P. Pushkarev, V. A. Ilichev, E. V. Baranov, T. A. Kovylina, and L. N. Bochkarev*
G.A. Razuvaev Institute of Organometallic Chemistry, Russian Academy of Sciences,
ul. Tropinina 49, Nizhny Novgorod, 603600 Russia
**e-mail: lnb@iomc.ras.ru*

Received December 8, 2016

Abstract—A new cyclometallated iridium(III) complex NBEpzIr(Piq)$_2$ (**I**) (NBEpzH is 1-phenyl-3-methyl-4-(5-bicyclo[2.2.1]hept-5-en-2-yl)-5-pyrazolone, PiqH is 1-phenylisoquinoline) is synthesized. The structure of the compound is determined by X-ray diffraction analysis (CIF file CCDC no. 1521037). Copolymers with the carbazole and iridium-containing fragments in the side chains (P1–P3) are prepared from monomer **I** by the ring-opening metathesis polymerization method. Their photoluminescence and electroluminescence properties are studied. Copolymers P1–P3 exhibit an intense photoluminescence and electroluminesce of red color. The maximum luminance (3010 cd/m^2) and current efficiency (15.1 cd/A) are achieved for emitter P2.

Keywords: iridium, cyclometallated complexes, iridium-containing polymers, metathesis polymerization, photoluminescence, electroluminescence

DOI: 10.1134/S107032841708005X

INTRODUCTION

The electroluminescent iridium-containing polymers are currently among the most efficient light-emitting polymeric materials for the fabrication of organic light-emitting diodes (OLEDs) of various applications [1]. Depending on the nature of the luminophoric iridium complexes linked to the polymer chain, the color of electroluminescence can vary from blue to red. The highest electroluminescence characteristics were achieved for the iridium-containing polymers emitting in the green spectral range [1]. The emitters with the red emission color are noticeably inferior to the “green” and “blue” iridium-containing polymers in electroluminescence efficiency. Therefore, the preparation of new more efficient iridium-containing polymers emitting in the red spectral range is an urgent task.

The synthesis and structure of the new cyclometallated iridium(III) complex NBEpzIr(Piq)$_2$ (**I**) (NBEpzH is 1-phenyl-3-methyl-4-(5-bicyclo[2.2.1]hept-5-en-2-yl)-5-pyrazolone, and PiqH is 1-phenylisoquinoline) and the preparation by the ring-opening metathesis polymerization (ROMP) method of related iridium-containing polymers P1–P3 with an intense photoluminescence (PL) and electroluminescence (EL) in the red spectral range are reported in this work.

EXPERIMENTAL

All procedures with readily oxidizable and hydrolyzable substances were carried out in vacuo or in argon using a standard Schlenk technique. The solvents used were thoroughly purified and degassed. Iridium(III) chloride [Ir(Piq)$_2$(Cl)]$_2$ [2], sodium pyrazolonate (NBEpz)Na [3], carbazole-containing monomer 9-(bicyclo[2.2.1]hept-5-en-2-ylmethyl)-9H-carbazole (L) [4], and (H$_2$IMes)(3-BrPy)$_2$(Cl)$_2$Ru=CHPh (third-generation Grubbs catalyst) [5, 6] were synthesized using known procedures. 4,7-Diphenyl-1,10-phenanthroline (BATH) and aluminum tris(8-oxyquinolinate) (Alq$_3$) (Aldrich) were used without additional purification.

^{1}H and ^{13}C{1H} NMR spectra were recorded on Bruker DPX-200 (^{1}H NMR: 200 MHz, ^{13}C NMR: 50 MHz) and Bruker Avance III-400 (^{1}H NMR: 400 MHz, ^{13}C NMR: 100 MHz) spectrometers, and signal assignment was performed using gradient 2D spectroscopy: proton–proton correlation (GE-COSY) and proton–carbon correlation (GE-HSQC). Chemical shifts are indicated in ppm relative to tetramethylsilane as an internal standard.

IR spectra were obtained on an FSM 1201 FT-IR spectrometer. A sample of compound **I** was prepared by pellet pressing with the substance to KBr ratio equal to 1 : 200. Samples of polymers P1–P3 were prepared as thin films between KBr plates.

The molecular weight distribution of the polymers was determined by gel permeation chromatography on a Knauer chromatograph with a Smartline RID 2300 differential refractometer as a detector and an array of two Phenomenex columns (Phenogel sorbent with a pore size of 10^4 and 10^5 Å) using THF as an eluent (2 mL/min) at 40°C. The columns were calibrated by 13 polystyrene standards.

The electronic absorption spectra of compound **I** and polymers P1–P3 in a CH_2Cl_2 solution were recorded on a Perkin Elmer Lambda 25 spectrometer. The PL spectra were obtained on a Perkin Elmer LS 55 fluorescence spectrometer. The relative quantum yields of complex **I** and P1–P3 were determined at room temperature in degassed solutions of CH_2Cl_2, and the excitation wavelength was $\lambda_{exc} = 360$ nm. The quantum yields were calculated relative to Rhodamine B in ethanol ($\Phi f = 0.70$) [7] according to an earlier described procedure [8].

Thermogravimetric analysis was carried out on a Perkin Elmer PYRIS 6 TGA thermogravimeter in a dry nitrogen flow (flow rate 80 cm^3/min, heating rate 5 K/min).

The EL spectra, current density–voltage and voltage–luminance characteristics, and chromaticity coordinates (CIE) were obtained on model OLED devices without encapsulation using an automated complex conjugated with a computer including a GW INSTEK PPE-3323 power source, a GW INSTEK GDM-8246 digital multimeter, and an Ocean Optics USB 2000 spectrofluorimeter.

Synthesis of NBEpzIr(Piq)$_2$ (I). A solution of (NBEpz)Na (0.05 g, 0.18 mmol) in DME (10 mL) was added to a solution of $(Ir(Piq)_2Cl)_2$ (0.10 g, 0.08 mmol) in DME (30 mL) in an argon atmosphere. The reaction mixture was refluxed for 24 h, cooled to room temperature, and centrifuged. The solvent was evaporated in vacuo, the solid residue was dissolved in dichloromethane (5 mL), and the solution was separated from a minor amount of a precipitate by centrifuging. After the solvent was removed under reduced pressure, the residue was dried in vacuo at 50°C for 4 h. The yield of complex **I** as an air-stable bright red finely crystalline substance was 0.09 g (68%).

IR (KBr), ν, cm^{-1}: 3075, 3043, 1154, 1115, 1071, 1047, 1002, 754, 738, 708 (C_{Ar}–H); 3043, 2962, 2926, 2860, 1478, 1370, 1350, 1311, 1269, 814 (C_{Alk}–H); 1605 ($C\cdots O$); 1576 ($C=C_{Ar}$); 1537 (C=N); 1433 (pyrazole ring); 932 (C–C); 613 (chelate ring); 477 (Ir–O).

According to the data of NMR spectroscopy, complex **I** was a mixture of *endo* and *exo* isomers.

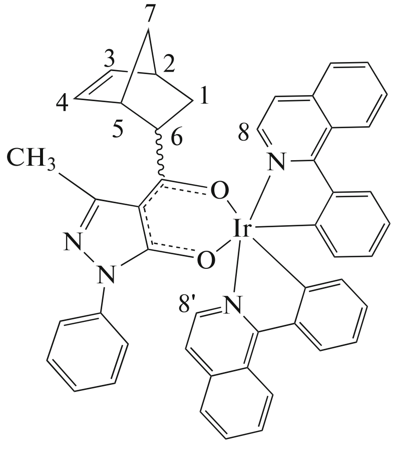

(I)

Endo isomer (80%). ^{1}H NMR ($CDCl_3$), δ, ppm: 8.99 (m, 2H, H^8, $H^{8'}$), 8.21 (dd, *J* = 18.8, 7.5 Hz, 3H, Ar), 7.90 (m, 1H, Ar), 7.84 (m, 1H, Ar), 7.70 (m, 8H, Ar), 7.43 (d, *J* = 4.7 Hz, 1H, Ar), 7.10 (dd, *J* = 13.7, 7.6 Hz, 2H, Ar), 6.95 (dd, *J* = 12.3, 6.3 Hz, 3H, Ar), 6.69 (t, *J* = 7.4 Hz, 2H, Ar), 6.49 (d, *J* = 7.4 Hz, 1H, Ar), 6.43 (d, *J* = 7.6 Hz, 1H, Ar), 5.45 (dd, *J* = 5.3, 2.6 Hz, 0.35H, H^3), 5.14 (dd, *J* = 5.1, 2.9 Hz, 0.65H, H^3), 5.06 (dd, *J* = 5.5, 2.8 Hz, 0.35H, H^4), 4.19 (dd, *J* = 5.4, 2.7 Hz, 0.65H, H^4), 3.49 (dd, *J* = 9.8, 6.2 Hz, 0.65H, H^6), 3.38 (m, 0.35H, H^6), 2.99 (s, 0.35H, H^2), 2.80 (s, 0.65H, H^5), 2.62 (s, 0.65H, H^2), 2.53 (s, 0.35H, H^5), 2.49 (s, 1.95H, Me), 2.47 (s, 1.05H, Me), 1.82 (m, 0.35H, H^1), 1.62 (m, 0.65H, H^1), 1.21 (m, 0.7H, H^7 and $H^{7'}$), 1.42 (s, 0.65H, $H^{1'}$), 1.19 (m, 0.65H, $H^{7'}$), 1.09 (s, 0.65H, $H^{7'}$), 0.64 (m, 0.35, $H^{1'}$).

Exo isomer (20%). ^{1}H NMR ($CDCl_3$), δ, ppm: 9.05 (m, 2H, H^8, $H^{8'}$), 8.61 (d, *J* = 6.4 Hz, 3H, Ar), 8.58 (d, *J* = 5.6 Hz, 1H, Ar), 8.49 (d, *J* = 6.4 Hz, 2H, Ar), 8.41 (d, *J* = 6.3 Hz, 2H, Ar), 8.34 (dd, *J* = 6.5, 3.5 Hz, 1H, Ar), 8.13 (d, *J* = 7.9 Hz, 2H, Ar), 7.92 (s, 1H, Ar), 7.88 (d, *J* = 3.0 Hz, 1H, Ar), 7.84 (s, 1H, Ar), 7.47 (s, 1H, Ar), 7.38 (s, 1H, Ar), 7.36 (s, 1H, Ar), 6.82 (t, *J* = 7.3 Hz, 2H, Ar), 6.55 (d, *J* = 6.6 Hz, 2H, Ar), 6.32 (dd, *J* = 5.5, 2.9 Hz, 1H, H3), 6.05 (d, *J* = 8.0 Hz, 2H, Ar), 5.88 (dd, *J* = 5.7, 2.8 Hz, 1H, H^4), 3.57 (m, 1H, H^6), 3.27 (s, 1H, H^5), 3.04 (s, 1H, H^2), 1.92 (m, 1H, H^1), 2.47 (s, 3H, Me), 1.55 (m, 1H, H^7), 1.48 (m, 1H, $H^{7'}$), 0.91 (m, 1H, $H^{1'}$).

All isomers. ^{13}C NMR ($CDCl_3$), δ, ppm: 193.9, 192.0, 169.6, 169.5, 169.1, 161.8, 162.0, 150.9, 150.7, 150.6, 149.9, 149.5, 147.6, 147.5, 147.0, 146.8, 146.4, 145.7, 143.8, 141.1, 140.8, 140.7, 140.6, 139.3, 138.6, 138.1, 137.3, 137.2, 137.1, 136.9, 136.3, 134.6, 134.3, 134.2, 134.0, 131.5, 131.2, 130.7, 130.3, 129.5, 129.1, 128.8, 128.4, 127.8, 127.6, 127.4, 127.3, 126.7, 126.6, 126.3, 126.1, 123.9, 121.0, 120.7, 120.5, 120.3, 119.9, 119.7, 119.5, 105.8, 105.5, 50.5, 49.8, 49.5, 49.3, 48.1, 47.9, 47.1, 46.6, 46.0, 43.3, 43.0, 42.4, 32.4, 31.1, 28.9, 28.3, 17.8, 17.4, 15.8.

For $C_{48}H_{37}N_4O_2Ir$

anal. calcd., %:	C, 64.48;	H, 4.17.
Found, %:	C, 64.58;	H, 4.23.

Synthesis of copolymer P1. The third-generation Grubbs catalyst (0.0027 g, 0.0031 mmol) in CH_2Cl_2 (1 mL) was added to a mixture of monomers **I** (0.0300 g, 0.0336 mmol) and L (0.0734 g, 0.2684 mmol) in CH_2Cl_2 (5 mL). The mixture was stirred at room temperature. The reaction course was monitored by thin layer chromatography. After the end of copolymerization (5 h), several droplets of vinyl ethyl ether was added to the reaction mixture to decompose the catalyst, and the mixture was stirred for 20 min. The formed copolymer was precipitated with methanol and dried in vacuo at room temperature to a constant weight. The yield of copolymer P1 as a red powder was 0.10 g (96%).

IR (KBr), ν, cm^{-1}: 3050, 1577, 1483, 1452, 1373, 1326, 1151, 1120, 1062, 1002, 748, 723 (C_{Ar}–H); 2940, 2868, 748 (C_{Alk}–H); 1596 (C···O); 1538 (C=C_{Ar}); 1538 (C=N); 1596 (pyrazole ring); 1625 (C=C); 1326, 1212, 908, 870 (C_{Alk}–C); 649, 618 (chelate ring); 565, 530 (Ir–O). ^{1}H NMR ($CDCl_3$), δ, ppm: 8.00 (m, 21H, Ar), 7.30 (m, 24H, Ar), 7.14 (m, 44H, Ar), 5.27 (m, 18H), 4.03 (m, 16H), 0.80–2.88 (m, 66H).

For $C_{208}H_{189}N_{12}O_2Ir$

anal. calcd., %:	C, 81.09;	H, 6.18.
Found, %:	C, 81.19;	H, 6.25.

M_w = 35800, M_n = 20000, M_w/M_n = 1.8, T_d = 332°C (at 5% weight loss).

Synthesis of copolymer P2 was carried out from compound **I** (0.0200 g, 0.0224 mmol) and L (0.0734 g, 0.2684 mmol) similarly to the procedure described for P1. The copolymerization time was 5 h. The yield was 0.09 g (97%).

IR (KBr), ν, cm^{-1}: 3050, 1577, 1483, 1461, 1452, 1383, 1326, 1152, 1121, 1062, 1001, 748, 722 (C_{Ar}–H); 2934, 2863, 819 (C_{Alk}–H); 1595 (C···O); 1577 (C=C_{Ar}); 1538 (C=N); 1538 (pyrazole ring); 1627 (C=C); 1326, 1212, 908 (C_{Alk}–C); 649 , 617 (chelate ring); 563, 529 (Ir–O). ^{1}H NMR ($CDCl_3$), δ, ppm: 7.99 (m, 33H, Ar), 7.31 (m, 37H, Ar), 7.14 (m, 51H, Ar), 5.26 (m, 26H), 4.02 (m, 24H), 0.60–3.10 (m, 94H).

For $C_{288}H_{265}N_{16}O_2Ir$

anal. calcd., %:	C, 82.86;	H, 6.40.
Found, %:	C, 82.97;	H, 6.47.

M_w = 36300, M_n = 22000, M_w/M_n = 1.7, T_d = 325°C (at 5% weight loss).

Synthesis of copolymer P3 was carried out from compound **I** (0.0150 g, 0.0168 mmol) and L (0.0734 g, 0.2684 mmol) similarly to the procedure described for P1. The copolymerization time was 5 h. The yield was 0.08 g (91%).

IR (KBr), ν, cm^{-1}: 3053, 1578, 1484, 1454, 1383, 1327, 1153, 1063, 1025, 749, 721 (C_{Ar}–H); 2929, 2865, 800 (C_{Alk}–H); 1598 (C···O); 1578 (C=C_{Ar}); 1539 (C=N); 1539 (pyrazole ring); 1628 (C=C); 1260, 1212, 909 (C_{Alk}–C); 649, 616 (chelate ring); 565, 529 (Ir–O). ^{1}H NMR ($CDCl_3$), δ, ppm: 8.01 (m, 38H, Ar), 7.31 (m, 52H, Ar), 7.14 (m, 63H, Ar), 5.27 (m, 34H), 4.05 (m, 32H), 0.70–2.80 (m, 122 H).

For $C_{368}H_{341}N_{20}O_2Ir$

anal. calcd., %:	C, 83.90;	H, 6.52.
Found, %:	C, 83.79;	H, 6.47.

M_w = 50700, M_n = 35000, M_w/M_n = 1.5, T_d = 310°C (at 5% weight loss).

X-ray diffraction analysis. The crystallographic data for compound **I** were collected on an Agilent Xcalibur E automated diffractometer (MoK_α radiation, λ = 0.71073 Å). Experimental arrays of intensities were integrated using the CrysAlisPro program [9]. The structure was solved by a direct method followed by the full-matrix least-squares refinement for F^2 (SHELXTL) [10]. An absorption correction was applied using the SCALE3 ABSPACK program [11]. All non-hydrogen atoms were refined in the anisotropic approximation, and hydrogen atoms were placed in the geometrically calculated positions and refined in the riding model. The norbornene substituent and Ph group of the pyrazolone ligand were disordered over two positions with the population ratios ~0.6 : 0.4 and 0.75 : 0.25, respectively. The six-membered fragment of the 1-phenylisoquinoline ligand was similarly disordered over two positions with the population ratio ~0.75 : 0.25. The crystal structure of complex **I** contains two solvate molecule of dichloromethane in the general positions falling onto one iridium complex. The crystallographic characteristics and the main refinement parameters are presented in Table 1.

The crystallographic information for compound **I** was deposited with the Cambridge Crystallographic Data Centre (CIF file CCDC no. 1521037; deposit@ccdc.cam.ac.uk or http://www.ccdc.cam.ac.uk).

Fabrication of OLED devices. A glass plate with the deposited ITO layer (ITO is indium–tin oxide, 120 nm, 15 Ohm/cm^2) (Lum Tec) acting as an anode was used as a support for OLED devices with the ITO/Ir-polymer (40 nm)/BATH (30 nm)/Alq_3 (30 nm)/Yb(150 nm) configuration. The emission layer of the copolymer was deposited from its solution in CH_2Cl_2 (6 mg/mL) on a Spincoat G3-8 centrifuge (3000 rpm, 30 s) and dried in vacuo at 70°C for 3 h. The layer thickness was determined with a META-900 ellipsometer. The hole-blocking BATH layer, electron-transporting Alq_3 layer, and Yb layer acting as a cathode were deposited by evaporation in vacuo (10^{-6} mmHg) from separate thermoresistant evaporators. The layer thickness was monitored with a calibrated quartz resonator. The active surface area of the devices was a square 5 × 5 mm in size.

RESULTS AND DISCUSSION

The iridium-containing polymers exhibiting the EL of red color contain the cyclometallated iridium(III) complexes with 2-(benzo[*b*]thiophen-2-yl)pyridiyl, 2-na-phthylpyridyl, 1-phenylisoquinoline, 2-phenylquinoline, 2,3-diphenylpyrazine, and 2,4-diphenylquinoline ligands in the main chain or in the side chains [1]. We have recently reported the preparation of the "red" electroluminescent polymers containing the iridium(III) complexes with the 2-(benzo[*b*]thiophen-2-yl)pyridiyl ligands in the side chains by ring-opening metathesis polymerization [12]. In this work, we synthesized the norbornene-containing cyclometallated iridium(III) complex with the 1-phenylisoquinoline ligands for the preparation of red-emitting polymers (Scheme 1).

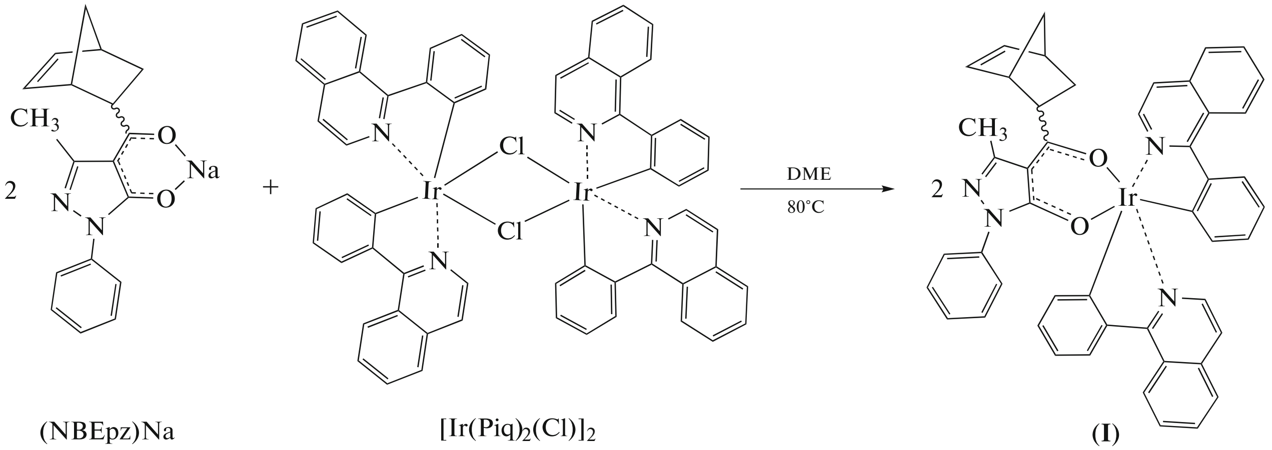

Scheme 1.

Complex **I** was synthesized in high yield as a bright red finely crystalline substance stable in air, soluble in $CHCl_3$, CH_2Cl_2, and DME, and insoluble in hexane. The NMR studies showed that the product was a mixture of *endo* and *exo* isomers with a ratio of 80 : 20.

The X-ray diffraction analysis of complex **I** showed that the single-crystal sample obtained after crystallization from dichloromethane contained only the *endo* isomer (Fig. 1, Table 2).

The iridium atom coordinates three chelate ligands: one pyrazolone ligand and two phenylisoquinoline ligands. The coordination polyhedron of the Ir atom is a distorted octahedron with the N(4), O(2), N(3), and C(33) atoms in the base and the axial positions occupied by the C(48) and O(1) atoms. The sum of bond angles between the equatorial substituents is 360°, and the C(48)Ir(1)O(1) angle is 176.3(2)°.

The pyrazolone ligand is coordinated to the Ir(1) atom by the O(1) and O(2) atoms. The Ir(1)–O(1,2) distances (2.166(4) and 2.168(4) Å, respectively) are close to similar distances in the related iridium complexes $(NBEpz)Ir(Ppy)_2$ [13] and $(NBEpz)Ir(Dfppy)_2$ [14] with two 2-phenylpyridine (Ppy) ligands and its fluorine-substituted analog (Dfppy) (2.142(2)–2.168(2) Å). The chelate O(1)Ir(1)O(2) angle (87.33(16)°) is close to similar angles in $(NBEpz)Ir(Ppy)_2$ (87.6(1)°) [13] and $(NBEpz)Ir(Dfppy)_2$ (87.9(1)°) [14]. The phenylisoquinoline ligands are coordinated to Ir(1) by the N(3), C(33), and N(4), C(48) atoms. The Ir–N and Ir–C bond lengths differ insignificantly (2.026(5), 2.027(5), and 1.979(6), 1.986(6) Å, respectively). Similar distances are observed in the related complex $(CBDK)Ir(Piq)_2$, where CBDK is 1-(carbazol-9-yl)-5,5-dimethylhexane-2,4-diketonate (2.028(3), 2.035(3) and 1.974(4), 1.991(4) Å) [15]. The chelate NIr(1)C angles of phenylisoquinolines in complex **I** (79.7(2)°, 80.1(2)°) are close to similar angles in $(CBDK)Ir(Piq)_2$ (79.53(15)°, 79.79(14)°) [15]. The phenylisoquinoline ligands are nonplanar, and the average shifts of the atoms from the plane are 0.08 and 0.21 Å. Similar values in complex $(CBDK)Ir(Piq)_2$ are 0.14 and 0.18 Å [15].

Luminophoric iridium complex **I** copolymerizes with carbazole-containing comonomer L and forms copolymers P1–P3 with different ratios of organic and metal-containing units (Scheme 2).

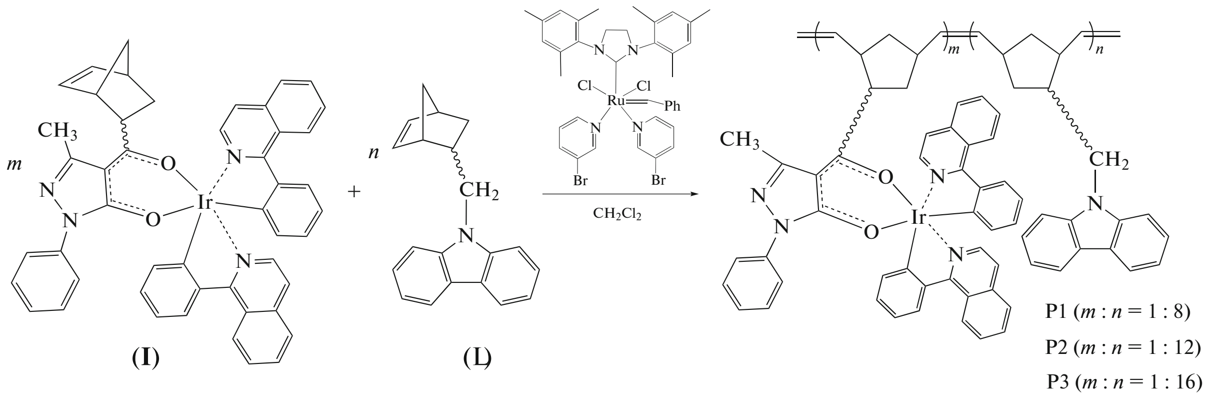

Scheme 2.

The ROMP reactions involving monomers **I** and L occur in the presence of the third-generation Grubbs catalyst at room temperature. The amount of the catalyst is 1 mol % with respect to the overall amount of the starting comonomers. It was determined by thin layer chromatography that the copolymerization processes completed within 5 h. Polymeric products P1–P3 were isolated as red powders stable in air and highly soluble in THF, CH_2Cl_2, and $CHCl_3$. The compositions of the copolymers were confirmed by elemental analysis and ^{1}H NMR spectroscopy.

It was found that the absorption spectrum of complex **I** (Fig. 2, Table 3) was similar to that of the known acetylacetonate iridium(III) complex $Ir(Piq)_2(Acac)$ [16]. The intense bands with maxima at 277, 342, and 356 nm in the spectrum of complex **I** are attributed to the intraligand $^1(\pi \to \pi^*)$ transitions in the 1-phenylisoquinoline and pyrazolonate ligands. The lower-intensity bands at 400–530 nm can be assigned to metal-to-ligand charge-transfer (MLCT) transitions [16]. Additional intense bands in a range of 260–350 nm caused by the $(\pi \to \pi^*)$ transitions in the carbazole fragments in addition to the bands characteristic of complex **I** are observed in the absorption spectra of copolymers P1–P3.

The PL spectrum of complex **I** (Fig. 3a) exhibits a band with a maximum at 614 nm and a lower-intensity band at 655 nm (shoulder to the main band) that can be assigned to the ^{3}LC and ^{3}MLCT transitions [16].

Table 1. Crystallographic data and X-ray diffraction experimental and refinement parameters for complex $\mathbf{I \cdot 2CH_2Cl_2}$

Parameter	Value
Empirical formula	$C_{50}H_{41}Cl_4IrN_4O_2$
FW	1063.87
Temperature, K	100(2)
Crystal system	Monoclinic
Space group	$P2_1/n$
a, Å	10.4468(2)
b, Å	14.7689(3)
c, Å	30.0049(5)
β, deg	97.387(2)
V, Å^3	4590.97(15)
Z	4
F(000)	2120
ρ_{calcd}, g cm^{-3}	1.539
μ, mm^{-1}	3.185
Crystal size, mm	0.40 × 0.20 × 0.20
Scan range over θ, deg	3.321–27.000
Ranges of indices	$-13 \le h \le 13$, $-18 \le k \le 18$, $-38 \le l \le 38$
Total number of reflections	76092
Number of independent reflections	9971
R_{int}	0.0774
GOOF (F^2)	1.062
R_1, wR_2 ($I > 2\sigma(I)$)	0.0552, 0.1202
R_1, wR_2 (all data)	0.0743, 0.1277
$\Delta\rho_{max}/\Delta\rho_{min}$, e Å^{-3}	1.398/–1.401

Table 2. Selected bond lengths (Å) and bond angles (deg) in complex **I**

Bond	d, Å	Angle	ω, deg
Ir(1)–O(1)	2.166(4)	O(1)Ir(1)O(2)	87.33(16)
Ir(1)–O(2)	2.168(4)	N(3)Ir(1)C(33)	80.1(2)
Ir(1)–N(3)	2.026(5)	N(4)Ir(1)C(48)	79.7(2)
Ir(1)–N(4)	2.027(5)	N(3)Ir(1)N(4)	174.9(2)
Ir(1)–C(33)	1.979(6)	O(1)Ir(1)C(48)	176.3(2)
Ir(1)–C(48)	1.986(6)	O(2)Ir(1)C(33)	174.8(2)
		N(4)Ir(1)O(2)	89.63(18)
		O(2)Ir(1)N(3)	95.01(19)
		C(33)Ir(1)N(4)	95.3(2)

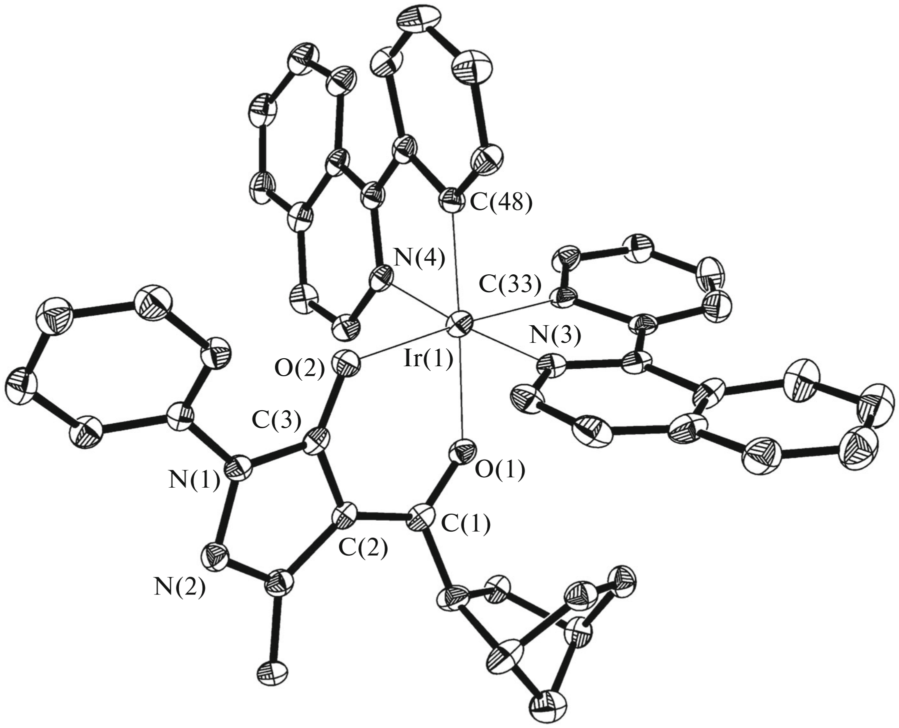

Fig. 1. Structure of complex **I** with ellipsoids of 30% probability. Hydrogen atoms are omitted.

Only the emission bands attributed to the ^{3}LC and ^{3}MLCT transitions in the iridium-containing fragments are observed in the PL spectra of copolymers P1–P3 in solutions and in thin films (Fig. 3, Table 3).

The PL quantum yields of copolymers P1–P3 are much lower than the quantum yield of monomer **I** (Table 3). Probably, this is associated with nonradiative losses in the polymer emitters caused by the diffusion of triplet excited states along the polymer chain and by triplet–triplet annihilation [17, 18].

The EL properties of copolymers P1–P3 were studied for the model OLED devices of the configurations ITO/Ir-polymer (40 nm)/BATH (30 nm)/Alq$_3$ (30 nm)/Yb. The EL spectra of the polymeric emitters

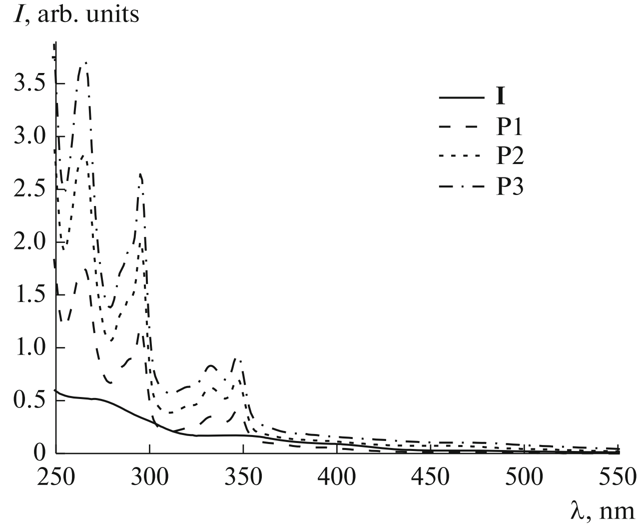

Fig. 2. Absorption spectra of complex **I** and polymers P1–P3 in a CH_2Cl_2 solution.

Table 3. Photophysical characteristics of complex **I** and polymers P1–P3

Compound	λ_{abs}, nm/log ε	λ_{em}, nm film	λ_{em}, nm CH_2Cl_2	PL quantum yield, % (CH_2Cl_2)
I	277 (3.76), 342 (3.40), 356 sh (3.26), 401 sh (3.00), 473 (2.48)		614, 655 sh	6.25
P1	264 (4.60), 284 sh (4.27), 289 sh (4.33), 295 (4.43), 319 sh (3.75), 332 (3.91), 346 (3.98), 367 sh (3.55), 393 sh (3.13), 464 sh (2.50), 494 (2.31)	617 sh, 627, 656 sh	616, 656 sh	2.64
P2	265 (4.95), 284 (4.61), 289 sh (4.66), 295 (4.80), 318 sh (4.14), 332 (4.30), 347 (4.34), 394 sh (3.57), 464 sh (3.35)	618 sh, 626, 657 sh	608, 650 sh	4.09
P3	265 (5.38), 283 sh (5.03), 289 sh (5.09), 295 (5.22), 320 sh (4.60), 332 (4.72), 347 (4.80), 394 sh (4.02), 474 sh (3.81)	622, 655 sh	617, 653 sh	5.58

Table 4. Performance characteristics* of the OLEDs based on polymers P1–P3

Polymer	Turn-on voltage, V**	Maximum luminance, cd/m^2	Maximum current efficiency, cd/A	Maximum power efficiency, lm/W	Chromaticity coordinates in CIE diagram
P1	7	1475 (30 V)	6.3 (12 V)	1.9 (9 V)	$x = 0.66$ $y = 0.33$
P2	6.5	3010 (30 V)	15.1 (11 V)	5.9 (7 V)	$x = 0.66$ $y = 0.34$
P3	7	2353 (30 V)	14.5 (8 V)	5.7 (8 V)	$x = 0.64$ $y = 0.35$

* The voltage at which the performance characteristics were determined is given in parentheses.
** Luminance at 1 cd/m^2.

and the performance characteristics of the related OLED devices are presented in Figs. 4 and 5 and in Table 4.

The EL spectra of copolymers P1–P3 are similar and contain bands with maxima in a range of 600–660 nm assigned to the ^{3}LC/^{3}MLCT transitions in the cyclometallated iridium complexes linked to the polymer chain. The absence of an emission from the carbazole groups at 350–450 nm indicates the efficient transfer of the excitation energy from the polymer matrix to the iridium-containing fragments via the Förster mechanism [19]. The chromaticity coordinates of the OLED emission in the CIE (Commision Internationale de l'Eclairage) diagram (Table 4) correspond to the red color and remain almost unchanged in the whole range of applied voltages. The highest luminance (3010 cd/m^2), current efficiency (15.1 cd/A), and power efficiency (5.9 lm/W) were shown by polymeric emitter P2. It should be mentioned that the achieved EL characteristics are comparable with similar characteristics of the known electroluminescent red-emitting iridium-containing polymers [1, 12, 20, 21].

To conclude, the new norbornene-containing cyclometallated iridium(III) complex was synthesized and structurally characterized. Carbon-chain copolymers P1–P3 with the carbazole and iridium-containing fragments in the side chains were prepared on the basis of the synthesized complex by the ROMP method. The obtained polymeric emitters exhibit the

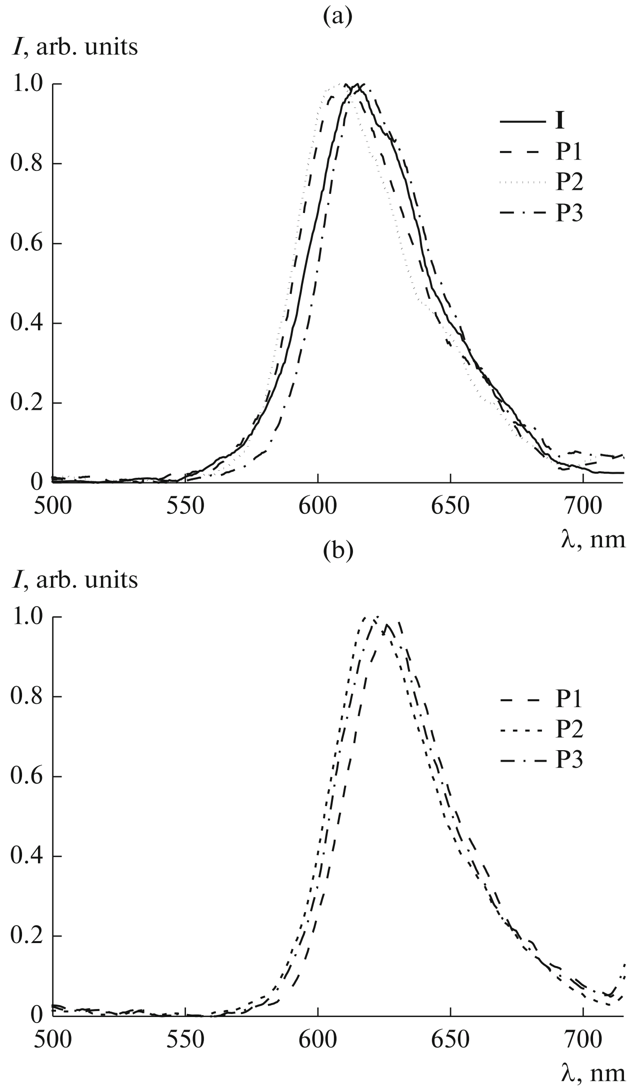

Fig. 3. Normalized photoluminescence spectra of (a) complex **I** and polymers P1–P3 in a CH_2Cl_2 solution and (b) polymers P1–P3 in film at room temperature (λ_{exc} = 360 nm).

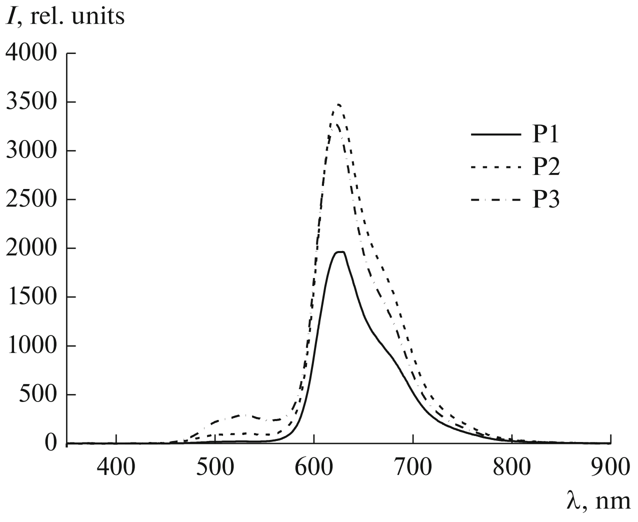

Fig. 4. Electroluminescence spectra of the OLEDs based on polymers P1–P3 at the maximum luminance.

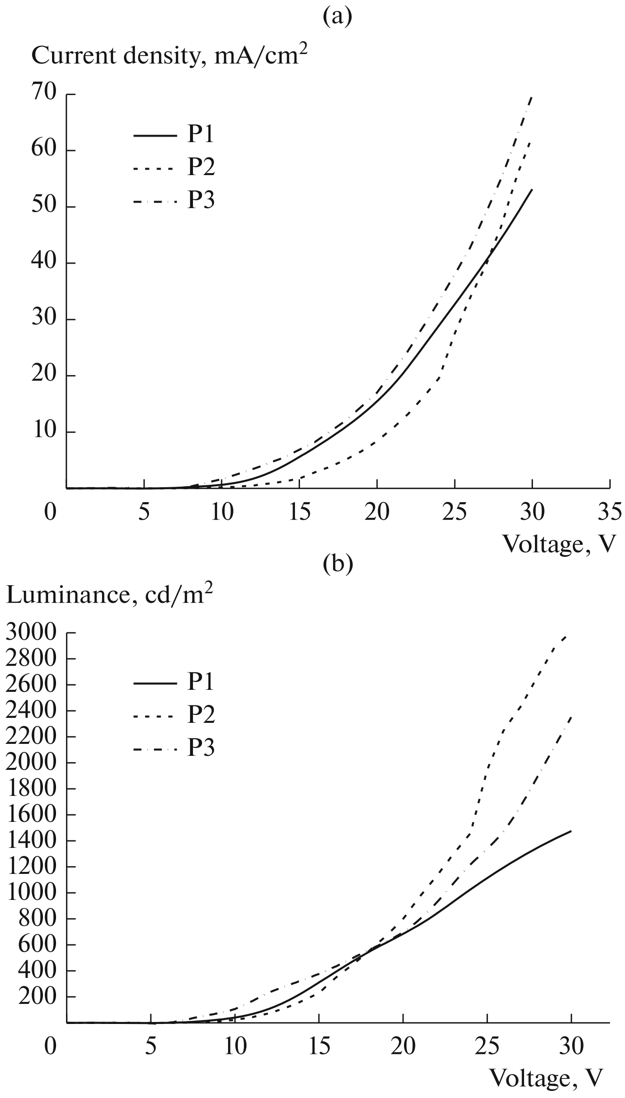

Fig. 5. (a) Current density–voltage and (b) voltage–luminance characteristics of the OLEDs based on polymers P1–P3.

intense photoluminescence and electroluminescence of red color. The maximum luminance (3010 cd/m^2), current efficiency (15.1 cd/A), and power efficiency (5.9 lm/W) were achieved by using emitter P2.

ACKNOWLEDGMENTS

This work was supported by the Russian Foundation for Basic Research (project nos. 16-33-00234-mol_a and 15-43-02178-r_povolzh'e_a).

REFERENCES

1. Xu, F., Kim, H.-U., Kim, J.-H., Jung, B.J., et al., *Prog. Polym. Sci.*, 2015, vol. 47, p. 92.
2. Lepeltier, M., Dumur, F., Marrot, J., et al., *Dalton Trans.*, 2013, vol. 42, p. 4479.

3. Begantsova, Y.E., Bochkarev, L.N., Malysheva, I.P., et al., *Synth. Met.*, 2011, vol. 161, p. 1043.
4. Liaw, D.-J. and Tsai, C.-H., *Polymer*, 2000, vol. 41, p. 2773.
5. Scholl, M., Ding, S., Lee, C.W., and Grubbs, R.H., *Org. Lett.*, 1999, vol. 1, p. 953.
6. Love, J.A., Morgan, J.P., Trnka, T.M., and Grubbs, R.H., *Angew. Chem., Int. Ed. Engl.*, 2002, vol. 41, p. 4035.
7. López Arbeloa, F., Ruiz, Ojeda, P., and López Arbeloa, I., *J. Lumin.*, 1989, p. 44, 105.
8. Demas, J.N. and Crosby, G.A., *J. Phys. Chem.*, 1971, vol. 75, p. 991.
9. *Data Collection. Reduction and Correction Program*, CrysalisPro-Software Package Agilent Technologies, 2012.
10. Sheldrick G.M., *SHELXTL. Version 6.14. Structure Determination Software Suite*, Madison: Bruker AXS Inc., 2003.
11. *SCALE3 ABSPACK. Empirical Absorption Correction*, CrysalisPro-Software Package Agilent Technologies, 2012.
12. Platonova, E.O., Il'ichev, V.A., Baranov, E.V., and Bochkarev, L.N., *Russ. J. Coord. Chem.*, 2016, vol. 42, no. 3, p. 187.
13. Begantsova, Yu.E., Bochkarev, L.N., Samsonov, M.A., and Fukin, G.K., *Russ. J. Coord. Chem.,* 2013, vol. 39, no. 9, p. 661.
14. Bochkarev, L.N., Begantsova, Yu.E., Il'ichev, V.A., et al., *Russ. J. Coord. Chem.*, 2015, vol. 41, no. 9, p. 555.
15. Ding, F., Bai, J., Chen, Z., et al., *Polyhedron*, 2013, vol. 52, p. 144.
16. Su, Y.-J., Huang, H.-L., Li, C.-L., et al., *Adv. Mater.*, 2003, vol. 15, p. 884.
17. Wilson, J.S., Chawdhury, N., Al-Mandhary, M.R.A., et al., *J. Am. Chem. Soc.*, 2001, vol. 123, p. 9412.
18. Partee, J., Frankevich, E.L., Uhlhorn, B., et al., *Phys. Rev. Lett.*, 1999, vol. 82, p. 3673.
19. Förster, T., *Disc. Farad. Soc.*, 1959, vol. 27, p. 7.
20. Park, J.H., Koh, T.W., Chung, J., et al., *Macromolecules*, 2013, vol. 46, p. 674.
21. Zhao, J., Lian, M., Yu, Y., et al., *Macromol. Rapid Commun.*, 2015, vol. 36, p. 71.

Translated by E. Yablonskaya